Controlled assembly of superparamagnetic iron oxide nanoparticles on electrospun PU nanofibrous membrane: A novel heat-generating substrate for magnetic hyperthermia application

ARTICLE *in* EUROPEAN POLYMER JOURNAL · DECEMBER 2013

Impact Factor: 3.01 · DOI: 10.1016/j.eurpolymj.2013.08.026

European Polymer Journal 49 (2013) 3796–3805

Contents lists available at ScienceDirect

European Polymer Journal

journal homepage: www.elsevier.com/locate/europolj

MACROMOLECULAR NANOTECHNOLOGY

Macromolecular Nanotechnology

Controlled assembly of superparamagnetic iron oxide nanoparticles on electrospun PU nanofibrous membrane: A novel heat-generating substrate for magnetic hyperthermia application

Altangerel Amarjargal [a,b,*], Leonard D. Tijing [c,d], Chan-Hee Park [a,*], Ik-Tae Im [c,*], Cheol Sang Kim [a,c,*]

[a] Department of Bionanosystem Engineering, Chonbuk National University, Jeonju, Jeonbuk 561-756, Republic of Korea
[b] Power Engineering School, Mongolian University of Science and Technology, Ulaanbaatar, Mongolia
[c] Division of Mechanical Design Engineering, Chonbuk National University, Jeonju, Jeonbuk 561-756, Republic of Korea
[d] School of Civil and Environmental Engineering, University of Technology, Sydney (UTS), P.O. Box 123, Broadway, NSW 2007, Australia

ARTICLE INFO

Article history:
Received 22 April 2013
Received in revised form 20 August 2013
Accepted 28 August 2013
Available online 12 September 2013

Keywords:
Fe_3O_4
Electrospun magnetic nanofiber
Hyperthermia

ABSTRACT

A facile method of fabricating novel heat-generating membranes composed of electrospun polyurethane (PU) nanofibers decorated with superparamagnetic iron oxide nanoparticles (NPs) is reported. Electrospinning was used to produce polymeric nanofibrous matrix, whereas polyol immersion technique allowed *in situ* assembly of well-dispersed Fe_3O_4 NPs on the nanofibrous membranes without any surfactant, and without sensitizing and stabilizing reagent. The assembly phenomena can be explained by the hydrogen-bonding interactions between the amide groups in the PU matrix and the hydroxyl groups capped on the surface of the Fe_3O_4 NPs. The prepared nanocomposite fibers showed acceptable magnetization value of 33.12 emu/g, after measuring the magnetic hysteresis loops using SQUID. Moreover, the inductive heating property of electrospun magnetic nanofibrous membranes under an alternating current (AC) magnetic field was investigated. We observed a progressive increase in the heating rate with the increase in the amount of magnetic Fe_3O_4 NPs in/on the membranes. The present electrospun magnetic nanofibrous membrane may be a potential candidate as a novel heat-generating substrate for localized hyperthermia cancer therapy.

1. Introduction

In recent years, with great attention to fusion technology, applications of nanomaterials have gained increasing interests to medical and biochemical fields. In particular, superparamagnetic nanoparticles with different kinds of nanostructures, have been the focus of many studies. This is because, the superparamagnetic nanoparticles do not retain any magnetization in the absence of a magnetic field, and thus have been widely used in magnetic resonance imaging, hyperthermia treatment of tumors, separation and purification of biomolecules, and targeted drug delivery [1–6]. Among the various magnetic nanoparticles, magnetite (Fe_3O_4) is one of the most important spinel-type particles with superparamagnetic property. It has been known that the important properties of Fe_3O_4 NPs for biomedical applications are nontoxicity, biocompatibility, low particle dimension, large surface area, and suitable

* Corresponding authors. Address: Department of Bionanosystem Engineering, Chonbuk National University, Jeonju, Jeonbuk 561-756, Republic of Korea. Tel.: +82 63 270 4284; fax: +82 63 270 2460 (C.S. Kim, A. Amarjargal). Fax: +82 63 270 2460 (I.T. Im).

E-mail addresses: a_amaraa1@jbnu.ac.kr, a_amaraa1@yahoo.com (A. Amarjargal), biochan@nate.com (C.-H. Park), itim@jbnu.ac.kr (I.-T. Im), chskim@jbnu.ac.kr (C.S. Kim).

0014-3057/$ - see front matter © 2013 Elsevier Ltd. All rights reserved.
http://dx.doi.org/10.1016/j.eurpolymj.2013.08.026

magnetic properties [7]. Combining magnetic NPs and polymeric matrices not only can lead to substantial enhancement in the surface chemistry for nanocomposites, but also polymers may serve as carrier for particles, as coating materials and encapsulating shell, as direct targeting and stabilizing agents, or as linker to couple functional biomolecules [8–14]. Yang et al. [10] have utilized diblock copolymers of poly(ethylene glycol) (PEG) and poly(3-caprolactone) (PCL) micelles to coencapsulate superparamagnetic iron oxide nanoparticles (SPIONPs) and an anticancer drug doxorubicin for dual targeting strategy (i.e. magnetic field-guided and ligand-directed targeting).

Superparamagnetic Fe_3O_4 NPs can be made to heat up in response to an alternating magnetic field, which leads to their use as hyperthermia agents, delivering toxic amounts of thermal energy (in the range of 41–45 °C) to tumors, where a moderate degree of tissue warming results in more effective cell destruction. Previous studies have suggested to use polymeric formulations to coat or encapsulate Fe_3O_4 NPs when they are used in magnetic fluid hyperthermia application, due to their improved physiochemical properties and biocompatibility [15,16]. Recently, Huang et al. [17] described the incorporation of IONPs into electrospun polystyrene fibers for the purpose of developing novel mediators for magnetic hyperthermia as an anti-cancer strategy. They suggested that the use of electrospun fibers for the encapsulation of IONPs has the additional advantage of fibers displaying a very high surface area over volume ratio, which may enhance their interactions with e.g., surrounding cells and the possible use of coated fibers for cell binding applications. Owing to the very small dimension of NPs, electrospinning of nanofibers presents itself as a facile method to decorate or incorporate NPs on polymeric nanofibers to add functionality. To date, numerous magnetic particles including magnetite, cobalt ferrite, Fe/Pt, and Fe@FeO have been successfully encapsulated into polymeric nanofibers where the principle of electrospinning remains similar. Most of these previous studies focused primarily on the production and characterization of magnetic fibers [18–21]. However, studies taking advantage of the potential of local heat-generating capability of magnetic electrospun nanofiber composites upon application of alternating magnetic field for hyperthermia treatment are limited [17,22]. One study reports on a magnetic nanofiber that encapsulated magnetite NPs being used for cancer therapy, which was delivered by surgical or endoscopic methods precisely to the tumor site. To the best of our knowledge, the fabrication of electrospun polyurethane (PU) nanofibers decorated with superparamagnetic Fe_3O_4 NPs and their potential use as heat-generating substrates for magnetic hyperthermia application has not been reported yet. The aim of the present work was to prepare nanofibrous polymeric membranes with high saturation magnetization by decorating Fe_3O_4 NPs without aggregation by combining the methods of electrospinning and polyol immersion, in the absence of any surfactant or sensitizing and stabilizing reagent [23].

Polyurethanes are excellent potential materials for the construction of implantable medical components due to their exceptional mechanical properties and biocompatibility [24–26]. Hence, the nanocomposite PU in electrospun form is a promising candidate for polymeric cover of nonvascular stents, which is employed in order to inhibit the overgrowth of malignant tissues that could cause blockage of passageway such as in the case of esophageal cancer [27]. We expect that well-dispersed and controlled assembly of Fe_3O_4 NPs on nanofibers can provide more heating performance when applying an external alternating magnetic field, which may present an attractive alternative for local magnetic hyperthermia treatment of easily accessible tumors.

2. Experimental

2.1. Synthesis of Fe_3O_4 NPs

Superparamagnetic Fe_3O_4 NPs were prepared by modified precipitation method followed by hydrothermal treatment, using a simple steam autoclave. In brief, 0.5 g iron chloride tetrahydrate ($FeCl_2{\cdot}4H_2O$, Samchun Chemicals) and 0.01 g poly(vinylpyrrolidone) (PVP, Alfa Aesar, MW-58000) were dissolved in 25 ml de-ionized water (DW) and then 2.5 ml ammonia solution (NH_4OH, Showa), was injected to the mixture under vigorous stirring in air for 10 min, allowing the iron (II) to be oxidized. The suspension was transferred to a 50 ml sealed pressure vessel, followed by thermal treatment at 125 °C and 180 kPa, for 90 min. Finally, it was cooled down to room temperature and the synthesized composites were separated by vacuum filtration. Dark brown precipitate was subsequently washed by ethanol, and then dried at 60 °C.

2.2. Preparation of electrospun PU nanofibers

Neat polyurethane (10 wt.%) solution was prepared by dissolving appropriate amount of PU pellets (Skythane® X595A-11) in DMF/MEK (50/50, wt:wt.%, Showa) solvent solution. Electrospinning was carried out at an applied voltage of 11 kV, a tip-to-collector distance of 15 cm and a solution feed rate of 1 ml h^{-1} via a syringe pump [28]. During electrospinning, the nozzle (inner diameter = 0.51 mm) kept on moving laterally (i.e., back and forth) on its axis for a distance of 150 mm and a linear speed of 100 mm/min controlled by LabVIEW 9.0 (National Instruments). Four ml of PU solution was electrospun onto a grounded flat collector, which was perpendicularly-oriented to the nozzle. The whole electrospinning set-up was enclosed in a sealed chamber, which was maintained at room temperature (~25 °C) and at a relative humidity of 20–30%. After electrospinning, the PU nanofibrous mat was dried at 80 °C for 48 h to remove the residual solvents.

2.3. Fabrication of magnetic electrospun nanofibrous membranes

Controlled assembly of superparamagnetic Fe_3O_4 NPs on electrospun PU nanofiber membranes was performed using a facile polyol immersion technique which was similar to our previous report [23]. In a typical procedure, electrospun PU nanofibrous mats (5 cm × 5 cm) were immersed in 25 ml of a previously-prepared colloidal EG

solutions with various concentrations (ranging from 0.5 to 2 mg/ml) of superparamagnetic nanoparticles under vigorous shaking in an incubator shaker at 60 °C. Mat samples were taken out after 20 h of immersion, and were then thoroughly rinsed with (DW) and dried at 60 °C for 24 h. For ease of discussion, the magnetic nanofiber membranes immersed in colloidal EG solution containing Fe_3O_4 NPs at concentration 0.5, 1 and 2 mg/ml will be referred herein as $MNF_{0.5}$, MNF_1 and MNF_2, respectively.

2.4. Characterization

The surface structure and morphology of the present Fe_3O_4 NPs and Fe_3O_4/PU composite nanofibrous mats were studied by field emission scanning electron microscopy (FE-SEM, S-7400, Hitachi, Japan) and the elemental composition was checked using an energy dispersive spectrometer (EDS). The particle size and distribution were determined using a transmission electron microscope (TEM, JEOL JEM, Japan) at an accelerating voltage of 200 kV. X-ray powder diffraction (XRD) analysis was carried out by a Rigaku X-ray diffractometer (Cu Kα, λ = 1.54059 Å) over Bragg angles ranging from 20° to 80°. Surface state of samples was surveyed by X-ray photoelectron spectroscopy (XPS, AXIS-NOVA, Kratos, Inc.) with an Al Kα irradiation source. Each spectrum was calibrated against the binding energy (BE) for adventitious carbon detected in the C1s region (284.6 eV BE). FTIR spectra of the samples were obtained using a Paragon 1000 Spectrometer (Perkin Elmer). The signal resolution of the FTIR was 1 cm^{-1} and a minimum of 16 scans was obtained and averaged within the range of 400–4000 cm^{-1}. The magnetic properties (M–H curve) of the nanoparticles were measured at room temperature on an MPMS magnetometer made by Quantum Design Corporation.

2.5. Hyperthermia test

In the present study, the magnetic electrospun nanofibrous membranes were used as novel heat generating substrates for magnetic hyperthermia application. Fig. 1 shows a photograph of alternating magnetic field generator (OSH-120-B, OSUNG HITECH, Republic of Korea) and its schematic representation used in the present study. The diameter of the three-turning coil was 60 mm. The magnetic field strength and its frequency were 1 kA m^{-1} (approximately 12.57 Oe) and 368 kHz, respectively [29]. The power of the heating generator was 5 kW. The magnetic nanofiber membranes on the tube-like paper support were placed in the center of the coil and an alternating current (AC) magnetic field was applied to the support. To evaluate the heating characteristics of the magnetic nanofibrous membranes, type-K thermocouples (KINTEX) were used to measure their surface temperature. The thermocouples were connected to a real-time data acquisition system for recording temperatures every second using LabVIEW (National Instruments) program.

3. Results and discussion

3.1. Structural and morphological characterization

3.1.1. XRD and XPS analysis

The XRD spectra of Fe_3O_4 NPs and composite electrospun PU nanofiber membranes are shown in Fig. 2a. It is found that the positions and relative intensities of the reflection peak of Fe_3O_4 NPs, which contain neither crystalline hematite (α-Fe_2O_3) nor iron hydroxides agree well with standard diffraction card JCPDS 19-0629. For composite nanofibers, all characteristic peaks were the same as those of Fe_3O_4 nanoparticles, while the intensity of the diffraction peak decreased significantly due to the physical combination between Fe_3O_4 nanoparticles and PU nanofibers without chemical reaction. Since magnetite (Fe_3O_4) and maghemite (γ-Fe_2O_3) particles have an inverse spinel structure and have very similar XRD patterns, making it difficult to distinguish between the two phases of iron oxide, precise studies on the phase composition and oxidation (valence) state of the sample were required. To that end, X-ray photoelectron spectroscopy (XPS) was employed to demonstrate the composition and structure of iron oxides, because XPS is very sensitive to Fe^{2+} and Fe^{3+}cations. The high resolution XPS spectrum of Fe 2p (Fig. 2b) contains the doublet Fe $2p_{3/2}$ and Fe $2p_{1/2}$ with binding energy values of 711.0 and 724.4 eV, typical for magnetite [30]. Here, the Fe_3O_4 peaks shifted to high binding energy and broadened due to the dual iron oxidation states of Fe^{2+} and Fe^{3+} compared with γ-Fe_2O_3, which is in good agreement with those reported in literature [31,32]. The absence of shake-up satellite structures at the higher binding energy sides of the main peaks, which are used as fingerprints to identify the γ-Fe_2O_3, suggest that a pure phase of Fe_3O_4 is obtained by present simple method.

3.1.2. FE-SEM

To have the polymer fibers effectively loaded with Fe_3O_4 NPs, which is essential in magnetic hyperthermia applications where the amount of accessible sites is important, a large ratio of Fe_3O_4 NPs relative to the polymer is usually incorporated into the polymer solution [17,22]. In this case, it is particularly difficult to prepare homogeneously dispersed magnetic NPs in/on a polymer matrix by sol–gel method and electrospinning technique due to the differences in density and polarity of the NPs and polymer. To avoid the above mentioned drawbacks associated with agglomeration and of NPs, we used a facile polyol immersion technique that allows *in situ* assembly of well-dispersed Fe_3O_4 NPs on electrospun PU nanofibers. Fig. 3 shows the FESEM image of the PU nanofiber membranes before and after the decorating of Fe_3O_4 NPs. As is apparent from Fig. 3a and a′, the surface of neat PU nanofibers is relatively smooth and the ultra fine matrix of interlocking fibers with sub-micron sizes, high porosity, and randomly-ordered morphology was found. Statistical analysis showed fiber diameter in the range of 400–800 nm with an average fiber diameter of 520 ± 104 nm (data not shown). Fig. 3b–d is the FE-SEM images of the decorated PU nanofiber membranes under the typical immersion

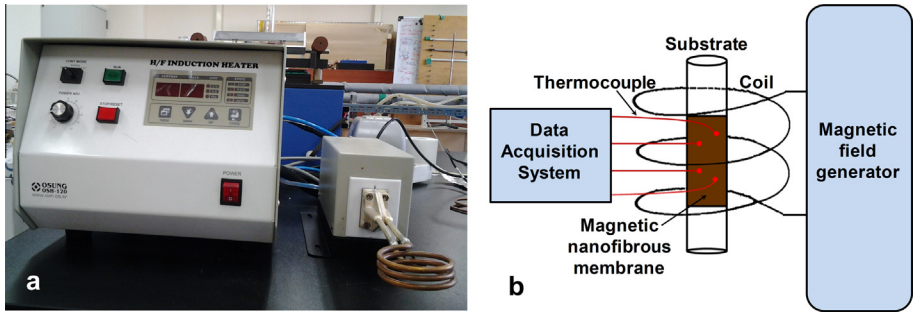

Fig. 1. (a) A photograph of the AC magnetic field generator. (b) Schematic representation field generator, coils, and a data acquisition system for recording temperatures.

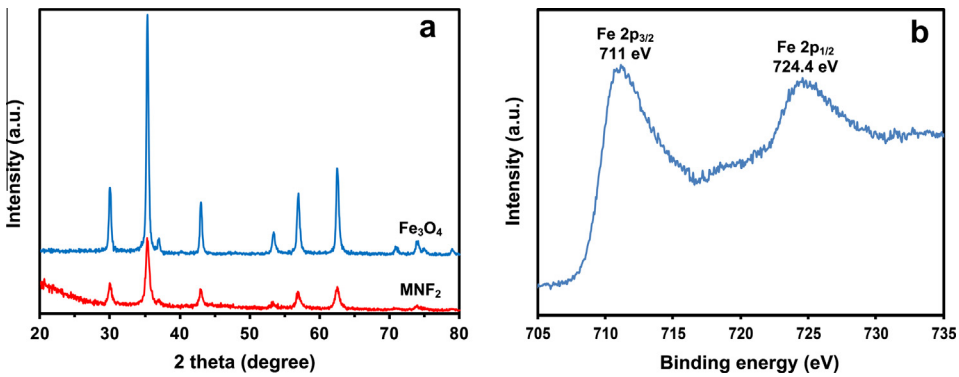

Fig. 2. XRD pattern (a) and Fe 2p (b) high resolution XPS spectra of Fe_3O_4 NPs.

conditions for 20 h. The porous structure of the PU nanofibrous membrane was not changed, while its relatively smooth surfaces were significantly roughened after the decoration of Fe_3O_4 NPs. From high magnification FE-SEM image of $MNF_{0.5}$ membranes (Fig. 3b′), it can be clearly seen that the Fe_3O_4 NPs are immobilized not only on the outer surfaces of PU nanofibers but also beneath the top layer of nanofibers. Once the immersion had progressed polyol solution with higher content of NPs, i.e., MNF_1 membranes (Fig. 3c′), the density of Fe_3O_4 NPs was further increased. Similarly, in case of MNF_2 membranes (Fig. 3d′), the surface of the PU nanofiber was completely covered by a sheath of densely packed Fe_3O_4 NPs. After the decoration of Fe_3O_4 NPs, the membrane turned from white to pale brown to deep brown as the concentration of NPs increased and maintained this color past several washings with water (insets of Fig. 3a–d).

3.1.3. Tem

TEM was employed to further observe the mean size of Fe_3O_4 NPs and its distribution over the PU nanofibers. As shown in Fig. 4a and b, the Fe_3O_4 NPs were found to be solid semi-spherical shape with narrow size distribution and the size was in range of 30–40 nm and no agglomeration occurs, indicating that the use of ferrous salt alone as the source material in basic aqueous under an elevated temperature and pressure can produce the formation of Fe_3O_4 NPs which is in accordance with the observation of Ge et al. [33]. Morphological differences in the nanofibers were depicted before and after the immersed with EG colloidal solution that contains Fe_3O_4 NPs at different concentrations by Fig. 4c–f. It showed that the neat PU nanofibers (Fig. 4c) do not contain any NPs before immersion treatment, whereas the nanocomposite fibers decorated with NPs (Fig 3d) were formed after immersion in the colloidal EG solution containing Fe_3O_4 NPs at concentration of 0.5 mg/ml. For the samples of MNF_1 and MNF_2, a large number of individual nanoparticles Fe_3O_4 are anchored strongly and distributed homogenously on the surface of nanofiber, unlike in previously reported cases where nanoparticles formed aggregates [22]. Judging from FESEM and TEM images, it should be noted that the coverage density of Fe_3O_4 NPs being assembled on the PU nanofibers is directly proportional to the amount of redispersed Fe_3O_4 NPs in a polyol medium. Generally, in order to functionalize surface of electrospun nanofibers with metal or metal oxide nanoparticles, many of reports were used the immersion technique followed by post treatment in the presence of surfactant, sensitizing and stabilizing reagent [34–36]. However, here, our PU nanofibers have been completely covered by a sheath of densely packed Fe_3O_4 NPs without using any additional chemicals to modify the nanofiber surfaces except of ethylene glycol dispersion medium. In the present study, the possible assembly mechanism for Fe_3O_4 NPs on the PU nanofibers could be explained on the basis of hydrogen bonding interactions

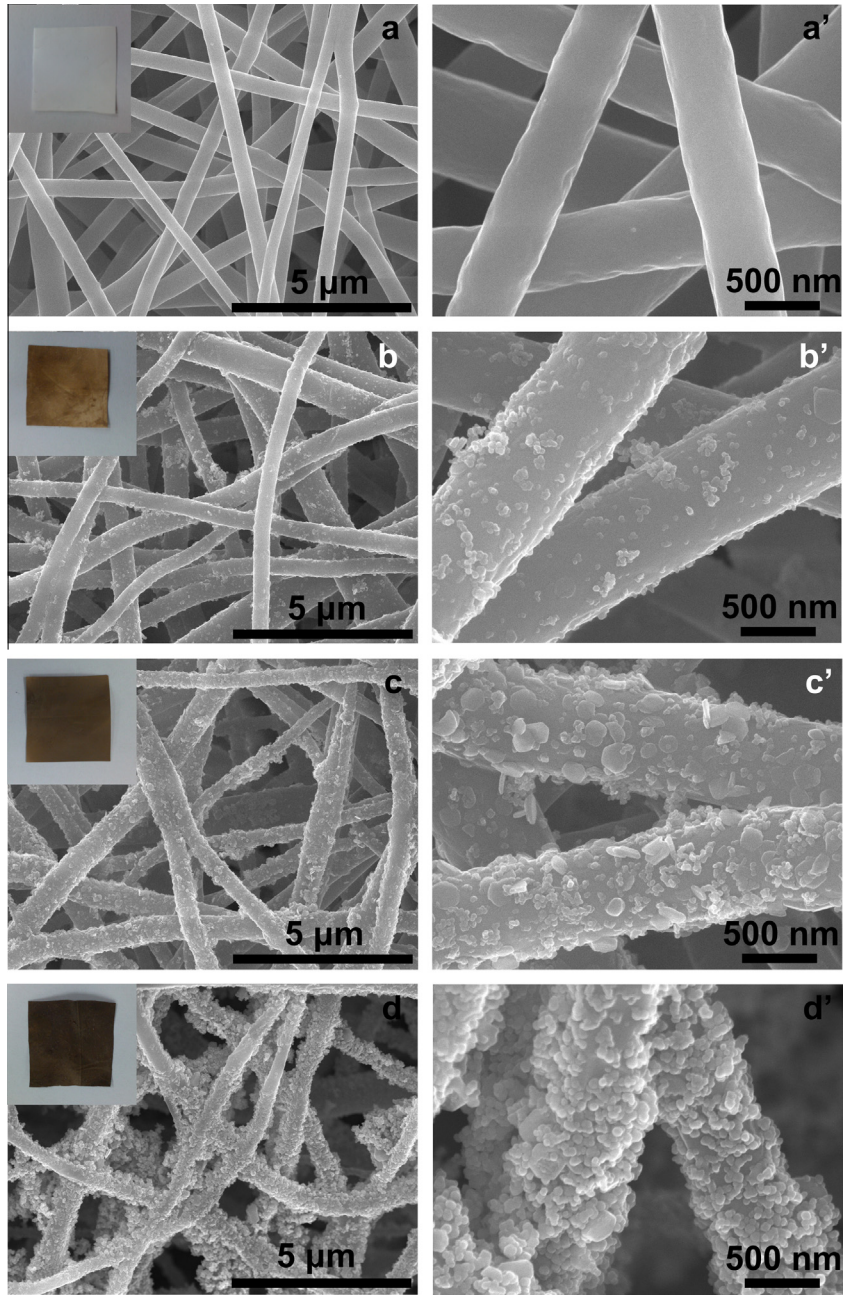

Fig. 3. The low- and high-magnification FE-SEM images of the electrospun neat and composite nanofiber membranes: (a and a′) PU; (b and b′) $MNF_{0.5}$; (c and c′) MNF_1; (d and d′) MNF_2. Photographs of each kind of membranes are added as insets in the corresponding FE-SEM images.

between the amide groups along the PU backbone and the hydroxyl groups capped on the surface of the Fe_3O_4 NPs [36].

3.1.4. FT-IR analysis

To characterize the molecular nature of a material, Fourier transform infrared (FT-IR) spectra of the samples were taken. As shown in Fig. 5a, a strong band at 539 cm^{-1} is assigned to the vibrational frequency due to the Fe—O bond. In addition, a broad and weak absorption peak was observed around 3347 cm^{-1}, which corresponds to O—H stretching vibration of H_2O in Fe_3O_4, that may have been caused by moisture absorption. On the other hand, the peaks for the neat PU nanofibrous mat in Fig. 5b can be assigned as follows: 3314 cm^{-1} (hydrogen bonded-NH stretching), 1729 cm^{-1} (free bonded >C=O (amide I band)), 1703 cm^{-1} (H-bonded >C=O (amide I region)) and 1596 cm^{-1} (C=C (benzene ring)). The absorption bands related to asymmetric and symmetric —CH_2 stretching are observed at 2944 and 2922 cm^{-1}, respectively, while vari-

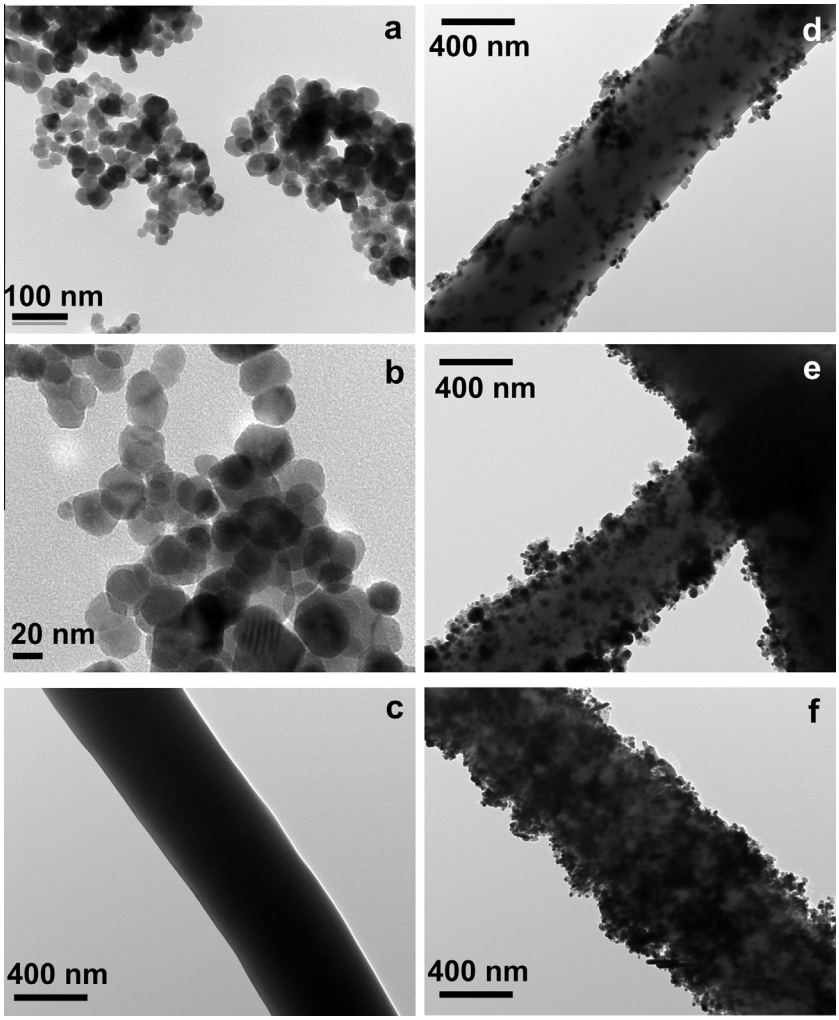

Fig. 4. Typical TEM images of Fe_3O_4 NPs at (a) low and (b) high magnification, an individual neat and composite nanofiber: (c) PU; (d) $MNF_{0.5}$; (e) MNF_1; and (f) MNF_2.

ous modes of —CH_2 vibrations are manifested in the range 1219–1413 cm^{-1} [37–40]. A comparison of the spectra in Fig. 5c shows the phenomenon that FTIR peaks for MNF_2 composites have been either shifted or appeared. For example, the characteristic peak corresponding to the stretching vibration of Fe—O bond did not only occur at 560 cm^{-1} as a new peak, but also was shifted to higher wavenumber compared to characteristic peak of Fe_3O_4 at 539 cm^{-1}. It is well known that the absorption peaks concerned with the amine (—NH—) and carbonyl (>C═O) groups are the main matter of consideration to evaluate the extensive intermolecular hydrogen bonding tendency of the PU matrix [40]. Correspondingly, a shifting of hydrogen bonded —NH absorption peak towards the higher wavelength region (peak shift of 11 cm^{-1}) in case of MNF_2 composites is present, which indicates that the majority of —NH groups in urethane linkages (—HN—COO—) participated in hydrogen bonding with the hydroxyl (—OH) group present in the Fe_3O_4 surface [41]. By measuring the peak intensity ratio of hydrogen bonded and free >C═O groups, it is possible to give an estimate of the degree of hydrogen bonding. Thus, the hydrogen bonding index, R, may be defined as the ratio of absorptions A_{1703}/A_{1729} [41,42]. The degree of phase separation (DPS) in the nanocomposites can be calculated from the peak intensity of these two bands following the equation:

$$\mathrm{DPS}\ (\%) = C_{\mathrm{bonded}}/(C_{\mathrm{bonded}} + C\ \mathrm{free}) \times 100,$$

where C is the concentration of the bonded and free carbonyl groups. Based on this calculation, the degree of phase separation ratio in neat PU nanofibers and MNF_2 composites is about 48% and 49.1%, respectively. This increase in the degree of phase separation ratio of MNF_2 composites may be due to the reaction of the hydroxyl (—OH) groups capped on the surface of the Fe_3O_4 NPs with the —NCO groups of the PU. Also, the greater strength of the hydrogen bonding between the —OH of Fe_3O_4 NPs and carbonyl group of urethane than intra-hydrogen bonding is attributed to this fact [41,43]. Moreover, the significant increase in intensity and slightly shifting towards

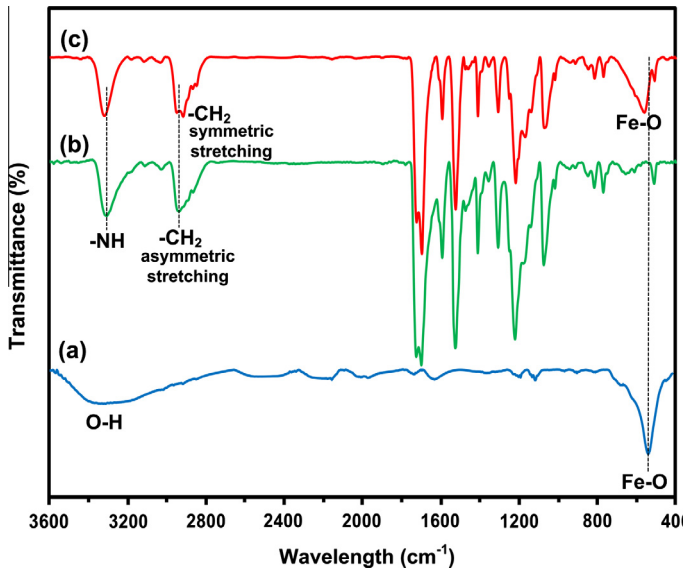

Fig. 5. FTIR spectra of (a) Fe_3O_4 NPs, (b) neat PU nanofibers and (c) MNF_2 membranes.

higher value of the peak at 2922 cm^{-1} and 2952 m^{-1} are associated with —CH_2 groups. These findings definitely confirm that a strong chemical bond exists between the organic polymer matrices and the inorganic metal oxides, which leads to the successful fabrication of magnetic composite mats. In addition to chemical bonding, the Fe_3O_4 NPs were applied onto nanofibers simply via physical adsorption by means of a polyol immersion technique.

3.2. Magnetic property

The magnetization–magnetic field (M–H) curves of samples were investigated with a SQUID magnetometer at 300 K by cycling the field between −10 and 10 k Oe as shown in Fig. 6. The Fe_3O_4 NPs displayed superparamagnetic property with a zero coercivity and a reversible hysteresis behavior (inset of Fig. 6), which gave a saturation magnetization value of 66.24 emu/g. In the case of magnetization curve for MNF_2, we observed a significant decrease in the saturation magnetization, which was only 33.12 emu/g, although it also exhibited superparamagnetic property. This decrease is attributed mainly to the presence of non-magnetic PU nanofibrous substrate. However, the values of the saturation magnetization for the MNF_2 membranes is still high compared with that of the polymer fibers containing iron oxide NPs reported by others, indicating that this value was much more acceptable for the application of hyperthermia [22,44–46]. As a natural result, our composite nanofibrous membrane showed field-responsive behavior with a magnet (inset of Fig. 6). As previous studies reported, saturation magnetization depended on the amount of iron oxide nanoparticles in the nanocomposites [44,47,48]. So, it should be noted that due to controlled assembly of Fe_3O_4 NPs on electrospun PU nanofibers, the magnetic properties of these well-fabricated membranes can easily be tuned by the amount of re-dispersed Fe_3O_4 NPs in an immersion medium.

3.3. In vitro hyperthermia measurements

In the next step, the heating performance of magnetic membranes made of the PU-Fe_3O_4 nanofibers, upon applying an alternating magnetic field, was studied. Fig. 7 shows the time-dependent heating curves for neat PU nanofibers and different magnetic electrospun membranes in the 368 kHz and 1 kA m^{-1} AC magnetic field. It was observed that the heating temperature for all the magnetic electrospun membranes increased with increasing time and it seems to reach equilibrium basically at the end of the test period. Also, a progressive increase in the heating rate was observed, as the amount of magnetic Fe_3O_4 NPs increases in the membranes, wherein the presence of magnetic Fe_3O_4 NPs was confirmed by morphological analysis. The MNF_2 membranes exhibited the fastest heating, reaching 41 °C in ~1 min. This magnetically-induced superior thermal response of the as-prepared nanomaterials indicate their hyperthermia feasibility under an AC magnetic field, owing to the energy released through the Néel relaxation process, which is the only mechanism contributing for superparamagnetic NPs assembled on electospun nanofibers.

In general, magnetic field-induced heating effect of iron oxide NPs usually proceed via two distinct mechanisms. The first one consists of the rotation of the single-domain particle, which is related to the Brownian motion of the magnetic particles. The second one corresponds to magnetization vector rotation if we abstract the Brownian motion and consider the particle immobile. The second one is the so-called Néel relaxation of fine magnetic particles, as previously mentioned [49–51]. Ferrofluid can exhibit both of these mechanisms, each having the proper weight. Besides, as iron oxide NPs are strongly hydrophobic, causing them to aggregate in an aqueous environment, the precise underlying mechanism of heating by iron oxide NPs cannot be easily studied. It can however be suggested that as

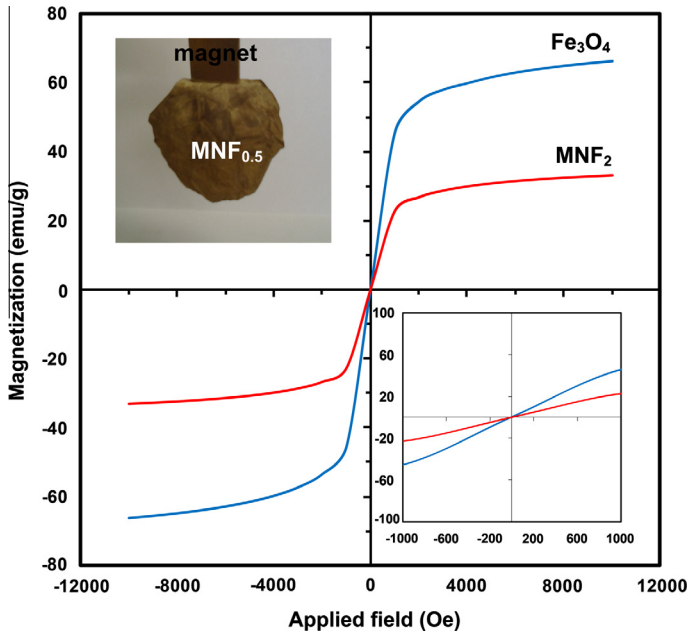

Fig. 6. Magnetic hysteresis loops of (a) Fe_3O_4 NPs and (b) MNF_2 membranes. The insets are the magnetic responsive images of $MNF_{0.5}$ membranes and magnified hysteresis loops.

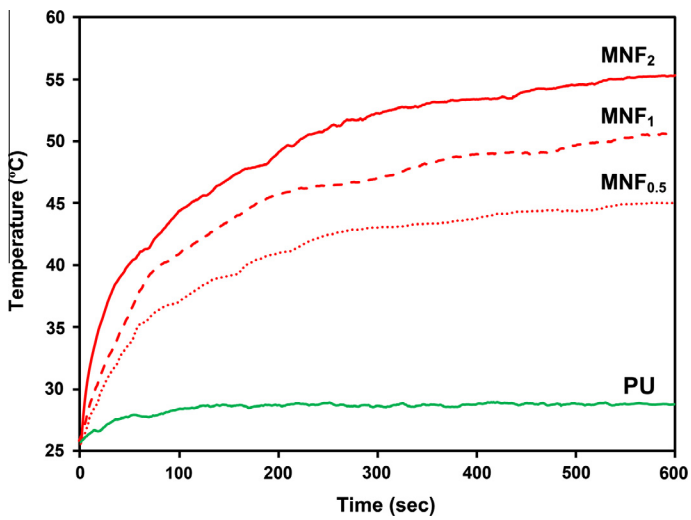

Fig. 7. Time-dependent temperature curves for neat PU and magnetic nanofiber membranes in an alternating magnetic field.

Fe_3O_4 NPs are strongly anchored onto electrospun PU nanofibers, their Brownian relaxation is likely very limited, whereas the relatively large size of the Fe_3O_4 NPs (40 nm diameter) will favor hysteresis over Néel relaxation as the main mechanism of magnetic energy dissipation [52]. Taking into account the acquired results, it is evident that polymer fiber webs containing IONPs can be repeatedly heated without loss of heating capacity or release of IONPs [17]. In a related study, the magnetic nanoparticles immobilized/entrapped on/in chitosan nanofiber composites showed no cytotoxicity to HFL1 (human lung fibroblast) cells [22]. Therefore, the present electrospun PU nanofibers decorated with Fe_3O_4 NPs can be used as a heat generating substrates and it is also expected to cover the non-vascular stents with the final purpose to place them in the immediate vicinity of a tumor, which is employed in order to capture metastatic cancer cells and to kill them through local magnetic hyperthermia. Thus, our future work will focus on the fabrication of covered non-vascular stents coated with magnetic electrospun nanofiber membranes and its in vitro feasibility study for hyperthermia treatment of tumor cells. The key advantages of applying covered non-vascular stents coated with Fe_3O_4 NPs immobilized nanofibrous membranes somewhere in the body is the

not only fact that the superparamagnetic nanoparticles remain localized, but also it can be worked as limiting barrier to overgrow the tumor, hereby offering the ability to repeat the magnetic heating as well as improved effective lifespan of the device such as in the case of esophageal stent [27].

4. Conclusion

In this study, superparamagnetic Fe_3O_4 NPs were synthesized by modified precipitation method followed by hydrothermal treatment and were subsequently immobilized on electrospun PU nanofibers by simple immersion in polyol solution without the need of any binding agent or surfactant except hot ethylene glycol solution. By varying the concentration of Fe_3O_4 NPs which is re-dispersed in immersion medium, controlled assembly of Fe_3O_4 NPs on nanofibers are successfully achieved. Some FT-IR peaks for composite PU nanofibers have been either shifted or appeared due to the presence of strong chemical bond exists between the organic polymer matrices and the inorganic metal oxides. The magnetic nanofiber membranes had higher saturation magnetization and remarkable heating effect when applying an alternating magnetic field, which has great potential application in hyperthermia treatment.

Acknowledgments

A. Amarjargal acknowledges the support of a fund from "Chonbuk National University Grant Fellow Project-2012" (Research Professor Program). This research was supported by a grant from the Basic Science Research Program through the National Research Foundation of Korea (NRF) funded by the Ministry of Education, Science and Technology (Project nos. 2012-0001611 and 2012-013341), and also by a grant from the Ministry of Education, Science and Technology through the Leaders in Industry-University Cooperation (LinC) Project (Project no. 2012-C-0043-010111). We also would like to thank KBSI-Jeonju (Korea) for taking high-quality FESEM and KBSI-Seoul (Korea) for obtaining the magnetic properties of our samples.

References

[1] Sitharaman B, Kissell KR, Hartman KB, Tran LA, Baikalov A, Rusakova I, et al. Superparamagnetic gadonanotubes are high-performance MRI contrast agents. Chem Commun 2005;31:3915–7.
[2] Sonvico F, Mornet S, Vasseur S, Dubernet C, Jaillard D, Degrouard J, et al. Folate-conjugated iron oxide nanoparticles for solid tumor targeting as potential specific magnetic hyperthermia mediators: synthesis, physicochemical characterization, and in vitro experiments. Bioconjugate Chem 2005;16(5):1181–8.
[3] Cho HS, Dong ZY, Pauletti GM, Zhang JM, Xu H, Gu HC, et al. Fluorescent, superparamagnetic nanospheres for drug storage, targeting, and imaging: a multifunctional nanocarrier system for cancer diagnosis and treatment. ACS Nano 2010;4(9):5398–404.
[4] Lee KS, Lee IS. Decoration of superparamagnetic iron oxide nanoparticles with Ni^{2+}: agent to bind and separate histidine-tagged proteins. Chem Commun 2008;6:709–11.
[5] Zhao Y, Lu Y, Hu Y, Li JP, Dong LA, Lin LN, et al. Synthesis of superparamagnetic $CaCO_3$ mesocrystals for multistage delivery in cancer therapy. Small 2010;6(21):2436–42.
[6] Huang YJ, Liu MZ, Chen JC, Gao CM, Gong QY. A novel magnetic triple-responsive composite semi-IPN hydrogels for targeted and controlled drug delivery. Eur Polym J 2012;48(10):1734–44.
[7] Gupta AK, Gupta M. Synthesis and surface engineering of iron oxide nanoparticles for biomedical applications. Biomaterials 2005;26(18):3995–4021.
[8] Liao ZY, Wang HJ, Lv RC, Zhao PQ, Sun XZ, Wang S, et al. Polymeric liposomes-coated superparamagnetic iron oxide nanoparticles as contrast agent for targeted magnetic resonance imaging of cancer cells. Langmuir 2011;27(6):3100–5.
[9] Tassa C, Shaw SY, Weissleder R. Dextran-coated iron oxide nanoparticles: a versatile platform for targeted molecular imaging, molecular diagnostics, and therapy. Acc Chem Res 2011;44(10):842–52.
[10] Yang XQ, Chen YH, Yuan RX, Chen GH, Blanco E, Gao JM, et al. Folate-encoded and Fe_3O_4-loaded polymeric micelles for dual targeting of cancer cells. Polymer 2008;49(16):3477–85.
[11] Chen DY, Xia XW, Gu HW, Xu QF, Ge JF, Li YG, et al. PH-responsive polymeric carrier encapsulated magnetic nanoparticles for cancer targeted imaging and delivery. J Mater Chem 2011;21(34):12682–90.
[12] Zhang JL, Srivastava RS, Misra RDK. Core-shell magnetite nanoparticles surface encapsulated with smart stimuli-responsive polymer: synthesis, characterization, and LCST of viable drug-targeting delivery system. Langmuir 2007;23(11):6342–51.
[13] Shukoor MI, Natalio F, Ksenofontov V, Tahir MN, Eberhardt M, Theato P, et al. Double-stranded RNA polyinosinic–potycytidylic acid immobilized onto y-Fe_2O_3 nanoparticles by using a multifunctional polymeric linker. Small 2007;3(8):1374–8.
[14] Boyer C, Whittaker MR, Bulmus V, Liu JQ, Davis TP. The design and utility of polymer-stabilized iron-oxide nanoparticles for nanomedicine applications. NPG Asia Mater 2010;2(1):23–30.
[15] Laurent S, Dutz S, Hafeli UO, Mahmoudi M. Magnetic fluid hyperthermia: focus on superparamagnetic iron oxide nanoparticles. Adv Colloid Interface 2011;166(1–2):8–23.
[16] Khandhar AP, Ferguson RM, Simon JA, Krishnan KM. Tailored magnetic nanoparticles for optimizing magnetic fluid hyperthermia. J Biomed Mater Res A 2012;100A(3):728–37.
[17] Huang CB, Soenen SJ, Rejman J, Trekker J, Liu CX, Lagae L, et al. Magnetic electrospun fibers for cancer therapy. Adv Funct Mater 2012;22(12):2479–86.
[18] Chen IH, Wang CC, Chen CY. Fabrication and characterization of magnetic cobalt ferrite/polyacrylonitrile and cobalt ferrite/carbon nanofibers by electrospinning. Carbon 2010;48(3):604–11.
[19] Song T, Zhang YZ, Zhou TJ. Fabrication of magnetic composite nanofibers of poly(epsilon-caprolactone) with FePt nanoparticles by coaxial electrospinning. J Magn Magn Mater 2006;303(2):E286–9.
[20] Zhu JH, Wei SY, Rutman D, Haldolaarachchige N, Young DR, Guo ZH. Magnetic polyacrylonitrile-Fe@FeO nanocomposite fibers – electrospinning, stabilization and carbonization. Polymer 2011;52(13):2947–55.
[21] Mincheva R, Stoilova O, Penchev H, Ruskov T, Spirov I, Manolova N, et al. Synthesis of polymer-stabilized magnetic nanoparticles and fabrication of nanocomposite fibers thereof using electrospinning. Eur Polym J 2008;44(3):615–27.
[22] Lin TC, Lin FH, Lin JC. In vitro feasibility study of the use of a magnetic electrospun chitosan nanofiber composite for hyperthermia treatment of tumor cells. Acta Biomater 2012;8(7):2704–11.
[23] Amarjargal A, Tijing LD, Ruelo MTG, Lee DH, Kim CS. Facile synthesis and immobilization of Ag–TiO2 nanoparticles on electrospun PU nanofibers by polyol technique and simple immersion. Mater Chem Phys 2012;135(2–3):277–81.
[24] Santerre JP, Woodhouse K, Laroche G, Labow RS. Understanding the biodegradation of polyurethanes: from classical implants to tissue engineering materials. Biomaterials 2005;26(35):7457–70.
[25] Osman AF, Edwards GA, Schiller TL, Andriani Y, Jack KS, Morrow IC, et al. Structure–property relationships in biomedical thermoplastic polyurethane nanocomposites. Macromolecules 2012;45(1):198–210.
[26] Zanden C, Voinova M, Gold J, Morsdorf D, Bernhardt I, Liu JH. Surface characterisation of oxygen plasma treated electrospun polyurethane fibres and their interaction with red blood cells. Eur Polym J 2012;48(3):472–82.
[27] Park CG, Kim MH, Park M, Lee JE, Lee SH, Park JH, et al. Polymeric nanofiber coated esophageal stent for sustained delivery of an anticancer drug. Macromol Res 2011;19(11):1210–6.
[28] Tijing LD, Park C-H, Choi WL, Ruelo MTG, Amarjargal A, Pant HR, et al. Characterization and mechanical performance comparison of multiwalled carbon nanotube/polyurethane composites fabricated by electrospinning and solution casting. Compos B Eng 2012.
[29] Park H, Park HJ, Kim JA, Lee SH, Kim JH, Yoon J, et al. Inactivation of *Pseudomonas aeruginosa* PA01 biofilms by hyperthermia using superparamagnetic nanoparticles. J Microbiol Meth 2011;84(1):41–5.

[30] Yamashita T, Hayes P. Analysis of XPS spectra of Fe2+ and Fe3+ ions in oxide materials. Appl Surf Sci 2008;254(8):2441–9.
[31] Teng XW, Black D, Watkins NJ, Gao YL, Yang H. Platinum-maghemite core–shell nanoparticles using a sequential synthesis. Nano Lett 2003;3(2):261–4.
[32] Lu J, Jiao XL, Chen DR, Li W. Solvothermal Synthesis and Characterization of Fe_3O_4 and gamma-Fe_2O_3 Nanoplates. J Phys Chem C 2009;113(10):4012–7.
[33] Ge S, Shi XY, Sun K, Li CP, Uher C, Baker JR, et al. Facile hydrothermal synthesis of iron oxide nanoparticles with tunable magnetic properties. J Phys Chem C 2009;113(31):13593–9.
[34] Zhao PT, Fan JT. Electrospun nylon 6 fibrous membrane coated with rice-like TiO2 nanoparticles by an ultrasonic-assistance method. J Membrane Sci 2010;355(1–2):91–7.
[35] Formo E, Lee E, Campbell D, Xia YN. Functionalization of electrospun TiO2 nanofibers with Pt nanoparticles and nanowires for catalytic applications. Nano Lett 2008;8(2):668–72.
[36] Dong H, Wang D, Sun G, Hinestroza JP. Assembly of metal nanoparticles on electrospun nylon 6 nanofibers by control of interfacial hydrogen-bonding interactions. Chem Mater 2008; 20(21):6627–32.
[37] Stuart BH. Infrared spectroscopy: fundamentals and applications. New York: John Wiley & Sons; 2004.
[38] Liu HZ, Zheng SX. Polyurethane networks nanoreinforced by polyhedral oligorneric silsesquioxane. Macromol Rapid Commun 2005;26(3):196–200.
[39] Lai YS, Tsai CW, Yang HW, Wang GP, Wu KH. Structural and electrochemical properties of polyurethanes/polyhedral oligomeric silsesquioxanes (PU/POSS) hybrid coatings on aluminum alloys. Mater Chem Phys 2009;117(1):91–8.
[40] Barick AK, Tripathy DK. Effect of nanofiber on material properties of vapor-grown carbon nanofiber reinforced thermoplastic polyurethane (TPU/CNF) nanocomposites prepared by melt compounding. Compos Part a-Appl S 2010;41(10):1471–82.
[41] Deka H, Karak N. Vegetable oil-based hyperbranched thermosetting polyurethane/clay nanocomposites. Nanoscale Res Lett 2009;4(7): 758–65.
[42] Chen TK, Tien YI, Wei KH. Synthesis and characterization of novel segmented polyurethane/clay nanocomposites. Polymer 2000; 41(4):1345–53.
[43] Dai XH, Xu J, Guo XL, Lu YL, Shen DY, Zhao N, et al. Study on structure and orientation action of polyurethane nanocomposites. Macromolecules 2004;37(15):5615–23.
[44] Miyauchi M, Simmons TJ, Miao JJ, Gagner JE, Shriver ZH, Aich U, et al. Electrospun polyvinylpyrrolidone fibers with high concentrations of ferromagnetic and superparamagnetic nanoparticles. Acs Appl Mater Inter 2011;3(6):1958–64.
[45] Zhang H, Zhu GQ. One-step hydrothermal synthesis of magnetic Fe3O4 nanoparticles immobilized on polyamide fabric. Appl Surf Sci 2012;258(11):4952–9.
[46] Wang SH, Wang C, Zhang B, Sun ZY, Li ZY, Jiang XK, et al. Preparation of Fe3O4/PVA nanofibers via combining *in situ* composite with electrospinning. Mater Lett 2010;64(1):9–11.
[47] Tan ST, Wendorff JH, Pietzonka C, Jia ZH, Wang GQ. Biocompatible and biodegradable polymer nanofibers displaying superparamagnetic properties. ChemPhysChem 2005;6(8):1461–5.
[48] Lai KL, Jiang W, Tang JZ, Wu Y, He B, Wang G, et al. Superparamagnetic nano-composite scaffolds for promoting bone cell proliferation and defect reparation without a magnetic field. Rsc Adv 2012;2(33):13007–17.
[49] Neel ML. Essai dinterpretation des proprietes magnetiques du sesquioxyde de fer rhomboedrique. Ann Phys-Paris 1949;4(May-):249–68.
[50] Mornet S, Vasseur S, Grasset F, Duguet E. Magnetic nanoparticle design for medical diagnosis and therapy. J Mater Chem 2004; 14(14):2161–75.
[51] Ma M, Wu Y, Zhou H, Sun YK, Zhang Y, Gu N. Size dependence of specific power absorption of Fe_3O_4 particles in AC magnetic field. J Magn Magn Mater 2004;268(1–2):33–9.
[52] Fortin JP, Wilhelm C, Servais J, Menager C, Bacri JC, Gazeau F. Size-sorted anionic iron oxide nanomagnets as colloidal mediators for magnetic hyperthermia. J Am Chem Soc 2007;129(9):2628–35.